

High-Energy Electron Production by the Raman and $2\omega_{pe}$ Instabilities in a 1.064- μm -Laser-Produced Underdense Plasma

D. W. Phillion, E. M. Campbell, K. G. Estabrook, G. E. Phillips, and F. Ze

Lawrence Livermore National Laboratory, University of California, Livermore, California 94550

(Received 27 April 1982)

Experiments on an underdense plasma irradiated with high-intensity 1.064- μm laser light have demonstrated that instabilities operating near $\frac{1}{4}$ the critical electron density can produce high-energy electrons. Experimental conditions were as follows: 7000- \AA CH foil targets, $2.5 \times 10^{15} \text{ W/cm}^2$, 900 psec, 400- μm spot diameter. The $3\omega_0/2$ light and 40-keV x rays occurred simultaneously at $t = -120$ psec (laser peak at $t = 0$) and lasted only 300 psec full width at half maximum. Ten percent of the laser energy appeared as Raman light and 0.04% as $3\omega_0/2$ light.

PACS numbers: 52.35.Py, 52.35.Mw, 52.50.Jm

The plasmas created by laser irradiation of fusion targets are subject to many parametric instabilities, among them the Raman and $2\omega_{pe}$ instabilities,¹⁻⁵ both of which can produce energetic electrons and preheat the deuterium-tritium fuel. The Raman instability can reduce the absorption, and what absorption does occur for both instabilities occurs at lower densities, so that the hydrodynamic efficiency is reduced: The energy is mostly wasted heating the corona. Stimulated Raman scattering⁶⁻¹⁴ and the two-plasmon-decay¹⁴⁻¹⁸ ($2\omega_{pe}$) instability have been extensively studied both experimentally and computationally. Both are three-wave parametric instabilities in which an incident photon decays into either two plasmons ($2\omega_{pe}$ instability) or into a plasmon and a lower-frequency photon (stimulated Raman scattering). Both instabilities require resonance: The frequencies and wave vectors of the daughter waves must sum to equal those of the incident light wave. This has the consequence that the $2\omega_{pe}$ instability and also the Raman instability, for a given frequency Raman light wave, are restricted by the resonance condition to occur only over a small range of electron densities. The intensity threshold decreases and the saturation level increases as the plasma density scale length is increased.

Many high-gain target designs for 1- μm laser light will have density scale lengths of hundreds to thousands of vacuum wavelengths. Experimentally, the problem is to determine what the threshold and saturation behavior are and what distribution of energetic electrons is produced. In this paper, we show both that efficient Raman scattering is possible and that the parametric instabilities operating near quarter critical electron density produce energetic electrons.

In order to create a completely underdense plasma which was hot and had a long electron density scale length, 6900- \AA thick Formvar (CH) foils were exploded with a 900-psec full width at half maximum (FWHM) Gaussian, 1.064- μm laser pulse at intensities in the range of (2-3) $\times 10^{15} \text{ W/cm}^2$. The lower or upper cluster of ten Shiva beams were overlapped onto a spot of 400- μm diameter. The ten Shiva beams effectively synthesize an $f/1.5$, radially polarized beam. Both experiment and hydrodynamic simulations indicate that these foils went underdense early in the laser pulse.

The foils were stretched across 25- μm thick gold washers which were 2 mm in outer diameter and 0.9 mm in inner diameter. Gold was chosen as the material for the supporting washer in order to generate a detectable number of high-energy bremsstrahlung x rays.

The intent was to measure the scattering-light signatures of the Raman and two-plasmon-decay instabilities, including the amount and spectrum of the forward-scattered Raman light. The $3\omega_0/2$ light energy was measured by an array of photodiodes. Additional diagnostics included a high-energy ($h\nu < 350 \text{ keV}$) x-ray spectrometer and an optical and x-ray (OX) streak camera, which simultaneously records the intensities of the $3\omega_0/2$ light, the 30-70-keV x rays, and the incident 1.064- μm laser light.

The major experimental results we will be presenting are as follows: First, the $3\omega_0/2$ light was generated at the same time and with the same duration as the 40-keV distribution of hot electrons which was produced, demonstrating the importance of instabilities near $n_c/4$ in hot-electron production. Secondly, Raman scattering was surprisingly efficient. About 10% of the inci-

dent laser energy appeared as Raman light with wavelength longer than $1.5 \mu\text{m}$, most of which was in the backscatter direction. The spectrum of the forward-scattered Raman light in one experiment was centered at $2.05 \mu\text{m}$, for which the wave-breaking energy is about 100 keV.

The major experimental finding was made by the OX streak camera. The $3\omega_0/2$ light and 30–70-keV x rays occurred simultaneously and lasted only about $\frac{1}{3}$ the incident laser pulse width of 900 psec. The $3\omega_0/2$ light is indicative of electron-plasma waves near $n_c/4$, one quarter the critical electron density. The OX streak record for one foil experiment is shown in Fig. 1(a). The three images from left to right are the incident $1.064\text{-}\mu\text{m}$ fiducial, the $3/2\omega_0$ light, and the 30–

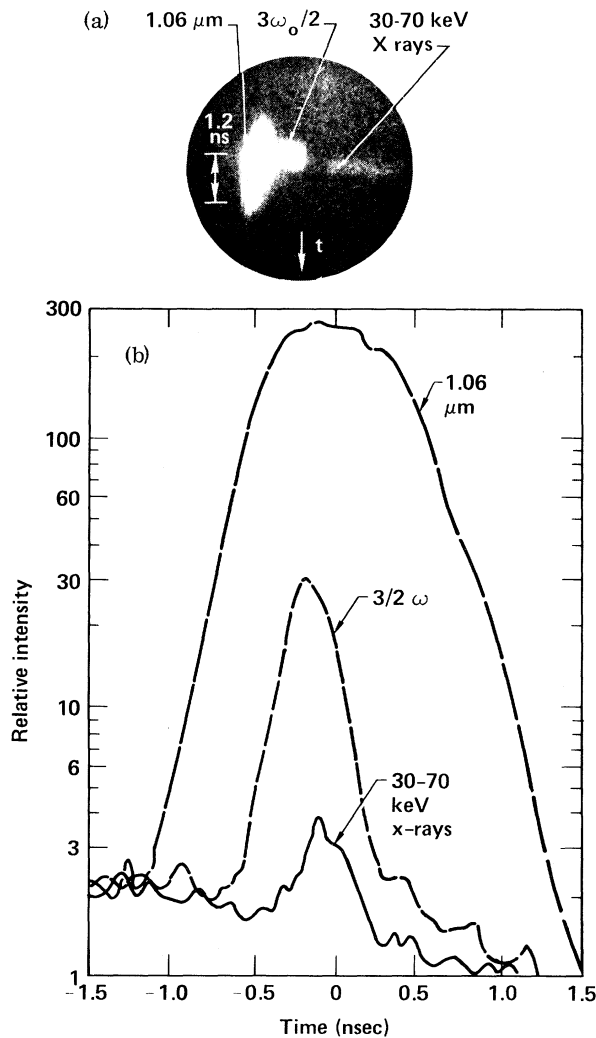


FIG. 1. (a) OX streak camera record. (b) Lineouts of the three images. The peak of the laser pulse is at $t = -40_{-50}^{+200}$ psec.

70-keV x rays, respectively. The $3\omega_0/2$ light seen by the OX streak camera was generated in the forward direction at 60° to the axis of the incident beams.

Lineouts of the three images are shown in Fig. 1(b). The peak of the laser pulse is at $t = -40_{-50}^{+200}$ psec, given that the fiducial is centered at $t = 0$. The FWHM of the fiducial is 980 psec which compares well with the 892 psec FWHM measured at the oscillator. The $3\omega_0/2$ light signal is 300 psec FWHM and the high-energy x-ray signal is 280 psec FWHM. The x rays are nearly coincident with the time of $3\omega_0/2$ emission: The x rays lag the $3\omega_0/2$ light by only 75 ± 25 psec. The peak of the $3\omega_0/2$ light emission is at $t = -160$ psec, which is 120_{-50}^{+200} psec before the peak of the laser pulse. This streak record establishes unequivocally the importance of quarter critical or near quarter critical electron densities in producing high-energy electrons. The high-energy x-ray spectrometer indicated that about 10 J of 40-keV electrons were stopped by the gold in these experiments. For both experiments, the slope of the superthermal x rays was about 40 keV, with a fluence of 4×10^{12} keV/keV at 84 keV and 4×10^9 keV/keV at 350 keV. Fluences are into 4π sr.

About 0.04% of the incident laser energy appeared as $3\omega_0/2$ light. The angular distribution was fairly isotropic, with about as much in the forward hemisphere as in the backward hemisphere. We have no measurement of the absorption fraction due to the $2\omega_{pe}$ instability, but particle code simulations indicate that it can be large.¹⁴

The angular distributions of the Raman light energy (Fig. 2) were measured by an array of light

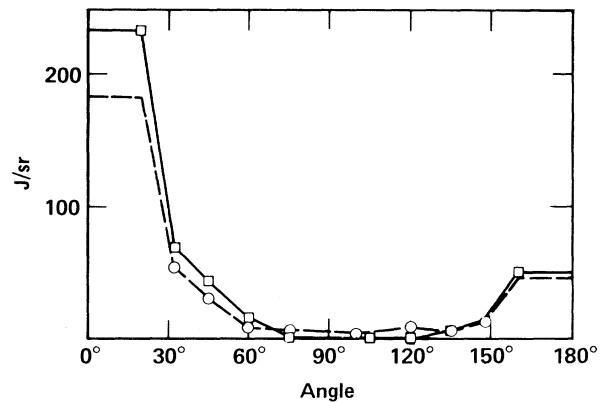


FIG. 2. Angular distribution of the Raman light energy. Squares, 2.5 kJ, 2.1×10^{15} W/cm². Circles, 3.1 kJ, 2.7×10^{15} W/cm². Direct backscatter is at $\theta = 0^\circ$.

calorimeters. The calorimeters are of the self-compensating, dual-receiver design with 1 mm NG-1 absorber glass. Each calorimeter has the Corning color filters 7-56 and 4-64, both of which are coated for 99.5% reflectivity at 1.064 μm and >80% transmission for the dielectric coating over the wavelength range $1.5 \mu\text{m} < \lambda < 2.6 \mu\text{m}$. A transmission of 30% through the filters has been assumed. The filter transmission depends on wavelength and is 42% at 2.0 μm , 30% at 1.8 μm , 18% at 1.6 μm , and 11.5% at 1.5 μm .

The integral under the solid curve in Fig. 2 is 325 J and for the dashed curve is 250 J. The 10% conversion efficiency into Raman light is the highest yet reported, but is not the first evidence that the Raman instability can be efficient. Offenberger *et al.*¹¹ measured 0.7% in experiments with a 10.6- μm CO₂ laser irradiating a magnetically confined plasma column. Other experiments¹² at 1.06 μm with solid targets have indicated probable efficiencies of several percent, although the Raman light intensity was measured at just one or two angles.

The forward-scattered Raman light spectrum shows a peak at 2.05 μm for both experiments (Fig. 3), but for the higher-intensity shot, there was also considerable forward-scattered Raman light at shorter wavelengths.

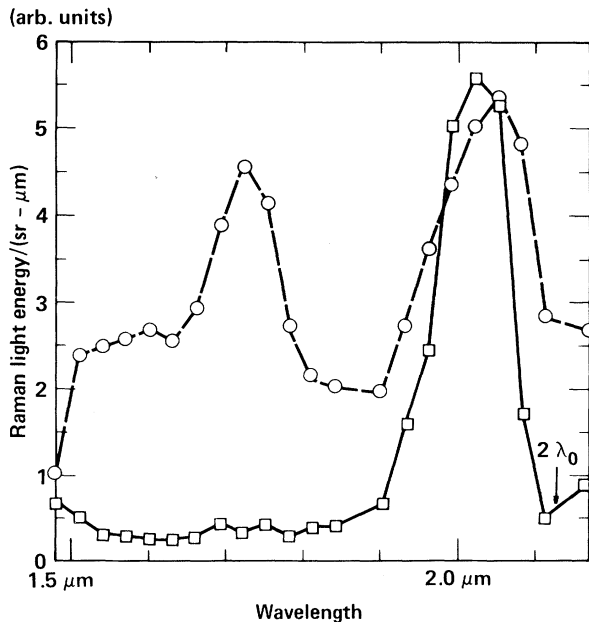


FIG. 3. Spectra of the forward-scattered Raman light. Squares, 2.5 kJ, 2.1×10^{15} W/cm², 45° away from forward. Circles, 3.1 kJ, 2.7×10^{15} W/cm², 20° from forward.

No measurements of electron density or temperature were made. That $\frac{2}{3}$ of the unabsorbed laser light was measured to be transmitted through the foil indicates that the foil went underdense early in the laser pulse. The absorption fraction was measured to be $(20 \pm 15)\%$ by an array of photodiodes. The fit $n_e = n_c [8.0(t + 0.88)]^{-1}$ describes to 10% accuracy for $|t| < 0.5$ ns the result of a two-dimensional hydrodynamic calculation for the on-axis peak electron density. The foil is calculated to go through $n_c/4$ at $t = -380$ psec and through $n_c/10$ at +370 psec. The plasma expands more to the front than the back. When the peak n_e was near $n_c/4$, the distance from $n_c/4$ to $n_c/8$ at the front was calculated to be 200 μm and to $n_c/16$ was 450 μm . The calculated absorption was 10% with the collisional absorption multiplier set to 2 and no modeling of laser-plasma instabilities. We have been able to do one-dimensional calculations with modeling of the Raman and Brillouin instabilities. These calculations indicated that 5% of the laser energy went into electron-plasma waves driven by the Raman instability, compared with 10% inferred from experiment. The density scale lengths calculated in one dimension were as much as a factor of 2 greater than in two dimensions.

The Raman instability was probably far above threshold in these experiments. From the Manley-Rowe relations, we know that the Raman instability must have caused about 10% of the incident light energy to go into electron plasma waves, since this amount appeared as Raman light and the frequencies of the electron plasma waves are comparable to those of the Raman light waves. Thus, about 20% of the incident laser light energy went either into the electron plasma waves or into the Raman light. Considering that the Raman instability was operative for only part of the laser pulse, this indicates that the Raman instability can be quite efficient when the threshold for convective instability is far exceeded. For instance, for $I = 3 \times 10^{15}$ W/cm², $n_e = 0.1n_c$, and direct backscatter, the Raman light wave convectively grows 20 intensity e -folding lengths for unpolarized light. These experiments show that the Raman instability may be important in laser-fusion schemes which use 1- μm light at high intensity ($> 10^{15}$ W/cm²).

We are grateful to Orville Barr and the Shiva operations crew for fitting these experiments into an already tight schedule and for working the needed extra hours. We also thank Lamar

Coleman for supporting these experiments.

This work was performed under the auspices of the U. S. Department of Energy by Lawrence Livermore National Laboratory under Contract No. W-7405-ENG-48.

¹C. S. Liu, in *Advances in Plasma Physics*, edited by A. Simon and W. B. Thompson (Wiley, New York, 1976), Vol. 6., p. 121.

²C. S. Liu, M. N. Rosenbluth, and R. B. White, *Phys. Fluids* **18**, 1002 (1975).

³D. W. Forslund, J. M. Kindel, and E. L. Lindman, *Phys. Fluids* **18**, 1017 (1974).

⁴J. F. Drake, P. K. Kaw, Y. C. Lee, G. Schmidt, C. S. Liu, and M. N. Rosenbluth, *Phys. Fluids* **17**, 778 (1974).

⁵C. S. Liu and M. N. Rosenbluth, *Phys. Fluids* **19**, 967 (1976).

⁶K. Tanaka, L. M. Goldman, M. C. Richardson, W. Seka, J. M. Soures, and E. A. Williams, *Phys. Rev. Lett.* **48**, 1179 (1982).

⁷J. Elazar, W. T. Toner, and E. R. Wooding, *Plasma*

Phys. **23**, 813 (1981).

⁸R. G. Watt, R. D. Brooks, and Z. A. Pietrzyk, *Phys. Rev. Lett.* **41**, 170 (1978).

⁹R. G. Watt and Z. A. Pietrzyk, *Appl. Phys. Lett.* **37**, 1068 (1980).

¹⁰J. L. Bobin, M. Decroisset, B. Meyer, and Y. Vitel, *Phys. Rev. Lett.* **30**, 594 (1973).

¹¹A. A. Offenberger, R. Fedosejevs, W. Tighe, and W. Rozmus, *Phys. Rev. Lett.* **49**, 371 (1982).

¹²D. W. Phillion, D. L. Banner, E. M. Campbell, R. E. Turner, and K. G. Estabrook, *Phys. Fluids* **25**, 1434 (1982).

¹³W. L. Kruer, K. G. Estabrook, B. F. Lasinski, and A. B. Langdon, *Phys. Fluids* **23**, 1326 (1980).

¹⁴K. G. Estabrook, W. L. Kruer, and B. F. Lasinski, *Phys. Rev. Lett.* **45**, 1399 (1980).

¹⁵H. A. Baldis, J. C. Samson, and P. B. Corkum, *Phys. Rev. Lett.* **41**, 1719 (1979).

¹⁶N. A. Ebrahim, H. A. Baldis, C. Joshi, and R. Benesch, *Phys. Rev. Lett.* **45**, 1179 (1980).

¹⁷H. A. Baldis and C. J. Walsh, *Phys. Rev. Lett.* **23**, 1658 (1981).

¹⁸A. B. Langdon, B. F. Lasinski, and W. L. Kruer, *Phys. Rev. Lett.* **43**, 133 (1979).

Regime of Improved Confinement and High Beta in Neutral-Beam-Heated Divertor Discharges of the ASDEX Tokamak

F. Wagner, G. Becker, K. Behringer, D. Campbell, A. Eberhagen, W. Engelhardt, G. Fussmann, O. Gehre, J. Gernhardt, G. v. Gierke, G. Haas, M. Huang,^(a) F. Karger, M. Keilhacker, O. Klüber, M. Kornherr, K. Lackner, G. Lisitano, G. G. Lister, H. M. Mayer, D. Meisel, E. R. Müller, H. Murmann, H. Niedermeyer, W. Poschenrieder, H. Rapp, H. Röhr, F. Schneider, G. Siller, E. Speth, A. Stäbler, K. H. Steuer, G. Venus, O. Vollmer, and Z. Yü^(a)

Max-Planck-Institut für Plasmaphysik, EURATOM-Association, D-8046 Garching, München, Germany
(Received 6 August 1982; revised manuscript received 1 October 1982)

A new operational regime has been observed in neutral-injection-heated ASDEX divertor discharges. This regime is characterized by high β_p values comparable to the aspect ratio A ($\beta_p \leq 0.65A$) and by confinement times close to those of Ohmic discharges. The high- β_p regime develops at an injection power ≥ 1.9 MW, a mean density $\bar{n}_e \geq 3 \times 10^{13}$ cm⁻³, and a $q(a)$ value ≥ 2.6 . Beyond these limits or in discharges with material limiter, low β_p values and reduced particle and energy confinement times are obtained compared to the Ohmic heating phase.

PACS numbers: 52.55.Gb, 52.50.Gj

One of the main goals in fusion-oriented tokamak research is the production and investigation of high-temperature, high- β plasmas. The stimulation for these efforts is the requirement of high β values for a fusion reactor device in order to achieve high fusion power output at low investments of magnetic field energy. A significant portion of the research program of all major tokamaks is devoted to the investigation of the

confinement properties of auxiliary-heated high- β tokamak plasmas.¹ ASDEX ($R = 165$ cm, $a = 40$ cm, toroidal field $B_T \leq 2.8$ T, plasma current $I_p \leq 0.5$ MA) is a divertor tokamak with neutral-beam injection (NI) presently capable of delivering 3.1 MW to the plasma for 200 msec at a source voltage of 40 kV. The power is delivered by two beam lines both oriented tangentially in the direction of the plasma current. Hydrogen

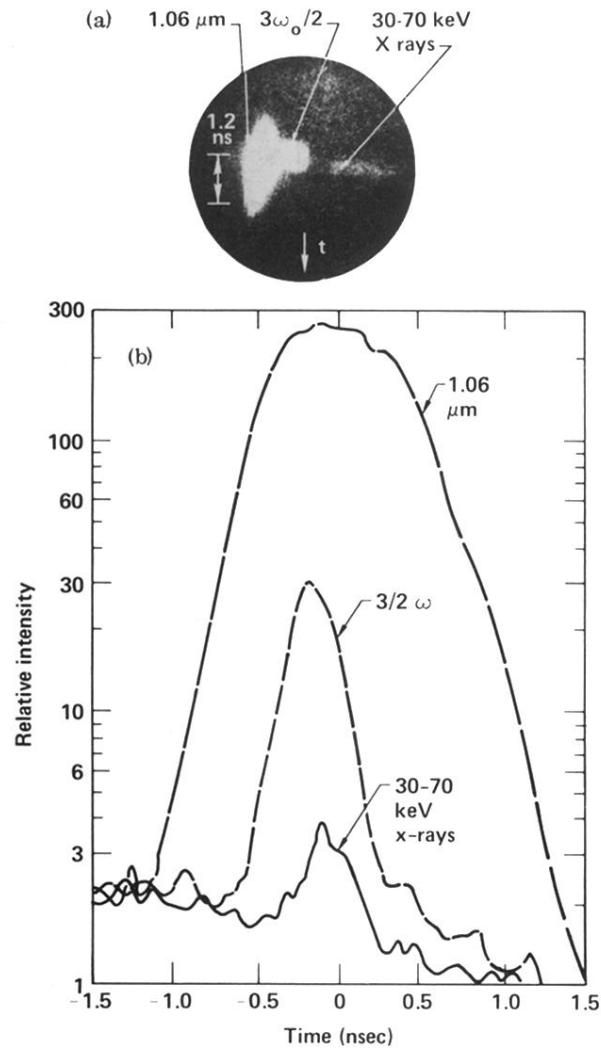


FIG. 1. (a) OX streak camera record. (b) Lineouts of the three images. The peak of the laser pulse is at $t = -40_{-50}^{+200}$ psec.